Theor Chem Acc (2012) 131:1103
DOI 10.1007/s00214-012-1103-4

REGULAR ARTICLE

Theoretical study on reaction mechanism of sulfuric acid and ammonia and hydration of $(NH_4)_2SO_4$

Wei-Wei Liu · Xiao-Lin Wang · Shi-Lu Chen · Yun-Hong Zhang · Ze-Sheng Li

Received: 2 June 2011 / Accepted: 24 October 2011 / Published online: 5 February 2012

Abstract In order to understand the mechanism of nucleation of $(NH_4)_2SO_4$ aerosol, the reaction between sulfuric acid and ammonia in the absence of water molecule is performed at M06/6-311++G(d,p) level. The results show that the $(NH_4)_2SO_4$ and NH_4HSO_4 units may exist instantaneously in gas phase without water molecule, which is a theoretical prediction that needs detection by further experiment. To further study the growth of the primary nuclei, the geometries, energies, and harmonic frequencies of $(NH_4)_2SO_4 \cdot (H_2O)_n$ ($n = 0$–9) are calculated both at M06/6-311++G(d,p) and B3LYP/6-311++G(d,p) levels. The tendency of the theoretical vibration frequencies is in accordance with the experimental results. The influence of the water molecule on the properties of $(NH_4)_2SO_4$ is also analyzed. Our results indicate that M06 is more accurate than B3LYP for this kind of system. Moreover, the first principle molecular dynamics method is used to simulate the structural transformation for two representative isomers whose energies are close, to understand the relationship between solvent-shared ion pairs and contact ion pairs.

W.-W. Liu · X.-L. Wang · S.-L. Chen · Y.-H. Zhang (✉) · Z.-S. Li (✉)
Key Laboratory of Cluster Science of Ministry of Education, School of Chemistry, The Institute for Chemical Physics, Beijing Institute of Technology, Beijing 100081, People's Republic of China
e-mail: yhz@bit.edu.cn

Z.-S. Li
e-mail: Zeshengli@bit.edu.cn

Z.-S. Li
Academy of Fundamental and Interdisciplinary Science, Harbin Institute of Technology, Harbin 150008, People's Republic of China

Keywords $(NH_4)_2SO_4$ · DFT · Molecular dynamics · Mechanism · Hydration

1 Introduction

One of the motivations for the interest in the hydrates of the ammonium sulfate is the presence in the atmosphere. The ammonium ion and sulfate ion involve in many chemical reactions, which are the most important ionic species of aerosols. These aerosols can alter climate by scattering radiation directly [1, 2] or act as cloud condensation nuclei [3]. The importance is more obvious in aqueous solutions where ion–solvent interactions involve hydrogen bond [4]. As for the nature of ion hydration bond, extensive experimental [5–12] and theoretical investigations [13–42] of cluster ions in the gas phase have been reported. Studies of the solvation clusters can provide molecular-level information of solute–solvent interactions by measuring the changes in energy, structure, and frequency as a function of the cluster size.

Using the electron diffraction method, ammonium sulfate and ammonium bisulfate were first observed in atmospheric aerosols by Friend et al. [43]. It is widely accepted that H_2SO_4 will rapidly react with NH_3 in the aqueous phase and yield $(NH_4)_2SO_4$ and NH_4HSO_4. But, there is a lack of information on whether they will take place in gas phase without water molecule. The intrinsic reaction mechanism in gas phase without solvent, if they can, is unknown. Thus, a theoretical study of the potential energy surface for this reaction is desirable. In this paper, we attempt to understand the possibility of $(NH_4)_2SO_4$ and NH_4HSO_4 existing in gas phase through the potential energy surface calculations. It is found that SO_4^{2-}, as a typical multiply charged anion not stable as isolated

species, can be stabilized by at least three hydrated water molecules in gas phase [44]. The effect of the water molecule on stabilizing this kind of system, $(NH_4)_2SO_4 \cdot (H_2O)_n$, should provide a comparison with $SO_4^{2-}(H_2O)_n$. Thus, we can infer that $(NH_4)_2SO_4$ also may be further stabilized by adding water molecules through analyzing the binding energies and structures too.

Based on the analysis of the hydrated $(NH_4)_2SO_4$, almost every NH_4^+ will form two hydrogen bonds with H_2O and one hydrogen bond with SO_4^{2-} as a proton acceptor. In these three hydrogen bonds, the hydrogen-bond distance between NH_4^+ and SO_4^{2-} is close to one of the others between NH_4^+ and H_2O, which indicates that the interaction between solute–solvent and solute–solute is similar in this system. The symmetric stretching frequencies of SO_4^{2-} are expected to be sensitive to the surrounding environment. However, the experimental spectrum [45] shows that there are rarely any changes of υ_1-SO_4^{2-} for $(NH_4)_2SO_4$ hydration system when the molar water-to-solute ratio decreases from 16.8 to 3.2, which is assigned to the similarity of the interactions among H_2O, NH_4^+, and SO_4^{2-}. Here, we utilize quantitative theoretical studies to reveal the mechanism and compare with experiment. We also discuss how gas species of $(NH_4)_2SO_4$ is stabilized by the stepwise attachment of outer shell water molecules to $(NH_4)_2SO_4$. Equilibrium structures, harmonic frequencies, and interaction energies of $(NH_4)_2SO_4 \cdot (H_2O)_n$ ($n = 0$–9) are performed using both M06 and B3LYP methods. The total and stepwise binding energies of the coupling are calculated. In addition, we want to get a suitable functional for this kind of system by comparing the M06 with the popular B3LYP method. Furthermore, we adopt the first principle molecular dynamics (MD) method to simulate the microscopic process of structural transformation for two representative isomers to understand the relationship between two different configurations. The time of hydrogen-bond replacement of NH_4^+–SO_4^{2-} by NH_4^+–H_2O and SO_4^{2-}–H_2O is consistent with the experimental results.

2 Computational methods

All calculations are carried out with GAUSSIAN 09 suite of programs [46]. The reaction between sulfuric acid and ammonia in the absence of water molecule is performed at M06/6-311++G(d,p) level, and the geometries of the reactants, products, intermediates, and transition states are optimized at the same level of theory. Both M06 [47] (DFT) and B3LYP [48] (DFT) are used to optimize the equilibrium structures of $(NH_4)_2SO_4 \cdot (H_2O)_n$ ($n = 0$–9) with 6-311++G(d,p) basis set. The final electronic relative energies are calculated using both 6-311++G(d,p) and Aug-cc-pvtz basis sets. We have attempted to locate several kinds of comparatively stable structures for every different species. However, it is more difficult to locate the most stable configurations for the larger clusters. We only display the most stable structures of $(NH_4)_2SO_4 \cdot (H_2O)_n$ ($n = 0$–2) and three comparatively stable structures of $(NH_4)_2SO_4 \cdot (H_2O)_n$ ($n = 3$–9) in our study, although other stable structures probably exist. Note that no super positional error (BSSE) is considered since it has been demonstrated that B3LYP and M06 methods almost have a negligible BSSE [47, 52]. It should be pointed out that a series of M06 approaches are applicable to deal with the non-covalent interactions [47, 53, 54].

Meanwhile, in order to further get the information about microscopic process of structural transformation among different isomers, the first principle MD method is used to simulate the structural transformation for two representative isomers whose energies are close. A side effect of evaluating force and energy by solving DFT equation is always the most computationally expensive. In our first principle MD, the exchange and correlation functionals are treated by Generalized Gradient Approximation (GGA) in the scheme of Perdew, Burke, and Erzerhof (PBE) [49] with DNP basis set. The simulation within 30 ps is performed under NVT thermodynamics ensemble at 298 K corresponding to the experiment used. The calculations are performed by the all electron density functional theory Dmol3 code [50, 51]. The equations of motion are integrated with a time step of 1 fs.

3 Results and discussion

3.1 Reaction mechanism of $(NH_4)_2SO_4$ in gas phase without water molecule

The potential energy surface for the reaction $H_2SO_4 + 2NH_3 \rightarrow (NH_4)_2SO_4$, including two transition states (TS1 and TS2) and one intermediate (NH_4HSO_4), obtained at M06/6-311++G(d,p) level of theory without the ZPE corrections in gas phase, is plotted in Fig. 1. The final product [$(NH_4)_2SO_4$] can be formed via the path: Reactant → TS1 → intermediate → TS2 → Product. As shown in Fig. 1, the energies of TS1, intermediate, TS2, and product are all higher than that of the reactant and lie at 5.53, 5.24, 13.60, and 13.52 kcal/mol, respectively. The energies of intermediate (NH_4HSO_4) and product are lower than those of TS1 and TS2 by only 0.29 and 0.08 kcal/mol, respectively, revealing that $(NH_4)_2SO_4$ and NH_4HSO_4 are located at the very shallow local minima in the potential energy surface. This means that both $(NH_4)_2SO_4$ and NH_4HSO_4 are very unstable. The total reaction enthalpies and free energies (12.71 and 14.24 kcal/mol, respectively, as

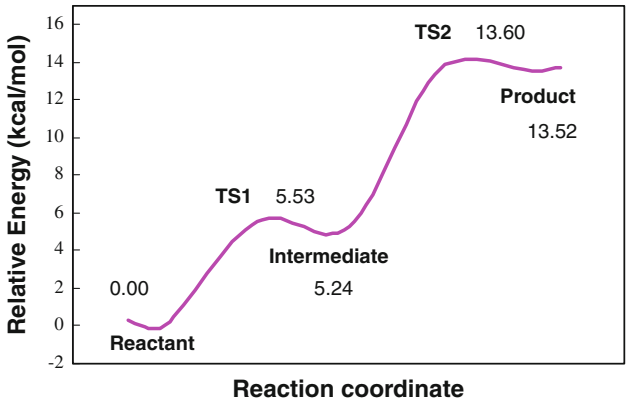

Fig. 1 Schematic potential energy surface of the $H_2SO_4 + 2NH_3$ reaction. Relative energies (kcal/mol) calculated at M06/6-311++G(d,p) level

Table 1 Calculated energy barriers, enthalpies, and free energies (kcal/mol) at M06/6-311++G(d,p) level under the conditions of 298.15 K and 1 atm

Reactions	ΔE	ΔH	ΔG
$2NH_3 + H_2SO_4 = NH_4HSO_4 + NH_3$	5.53	5.51	6.65
$NH_4HSO_4 + NH_3 = (NH_4)_2SO_4$	8.36	7.20	7.59
$2NH_3 + H_2SO_4 = (NH_4)_2SO_4$	13.60	12.71	14.24

listed in Table 1) indicate a very large endothermicity. Therefore, if the reaction takes place, the more rigorous reaction conditions such as higher temperature and pressure may be required in experiments.

It is very interesting to trace geometrical and charge distribution changes along the reaction pathway, since they may reflect important chemistry. In the reactant, the distances of the transferred hydrogen to the oxygen and the nitrogen (N_2) are 1.013 and 1.706 Å, respectively (Fig. 2). They are changed to 1.608 and 1.074 Å in the intermediate, via 1.406 and 1.139 Å at TS1. The observed similar geometries between TS1 and the intermediate give a clear indication that TS1 is a very late transition state, a conclusion that is also consistent with the energetics described above, that is, TS1 and the intermediate are very close in energy. Simultaneously with the hydrogen delivered from the oxygen to the nitrogen, the negative charge at the oxygen is increased while the nitrogen becomes less negatively charged (Fig. 2). This implies that the step in going from the reactant to the intermediate via TS1 is a proton-transfer process. The changes of geometrical and electronic parameters in the second step (from the intermediate to the product via TS2, Fig. 2) reveal the same nature, that is, an endothermic proton-transfer process.

3.2 Structures and relative energies

A series of equilibrium structures of gas-phase hydrated ammonium sulfate, $(NH_4)_2SO_4 \cdot (H_2O)_n$ ($n = 0$–9), are obtained using density functional methods. Some representative stable structures of $(NH_4)_2SO_4 \cdot (H_2O)_n$ ($n = 0$–9) calculated at the theory level of M06/6-311++G(d,p) are listed in Figs. 3 and 4. It should be noted that the structures of $(NH_4)_2SO_4$ and $(NH_4)_2SO_4 \cdot H_2O$ (1I) can be obtained with the M06/6-311++G(d,p) calculations but the attempts to optimize the same structures at B3LYP/6-311++G(d,p) level always failed. The relative energies of optimized structures at different theory levels are presented in Table 2. The energy of the most stable one among structures with the same number of water molecules is set to zero (see Table 2). The average hydrogen-bond distances of the isomers for $(NH_4)_2SO_4 \cdot (H_2O)_n$ ($n = 2$–9), R (NH_4^+–SO_4^{2-}) and R (NH_4^+–H_2O), are listed in Fig. 5. The structures of clusters are constructed by adding water molecule to $(NH_4)_2SO_4$ gradually, and their main properties will be discussed as follows.

$(NH_4)_2SO_4$: The geometry of $(NH_4)_2SO_4$ in gas phase was optimized at the M06/6-311++G(d,p) level and is

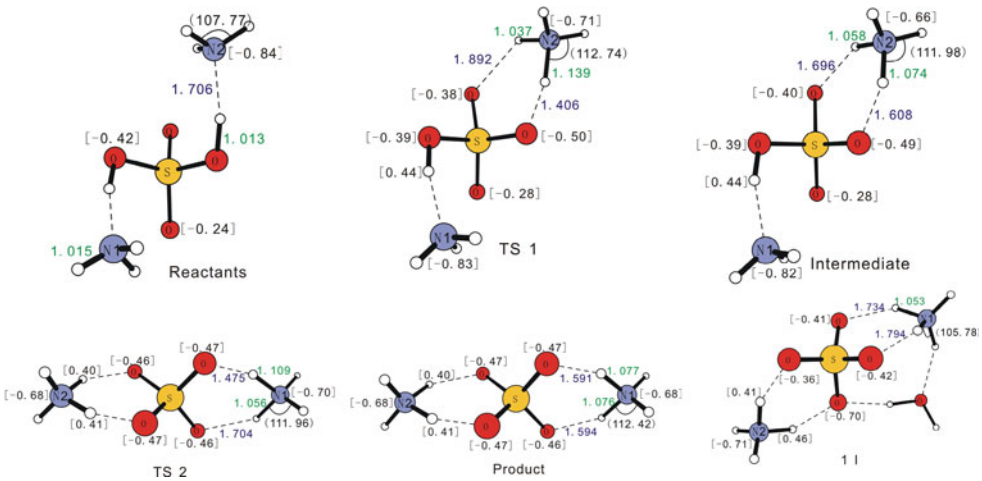

Fig. 2 Partial charges, bond length, hydrogen-bond distances and angle of reactants, intermediate, transition states, product, and $(NH_4)_2SO_4 \cdot (H_2O)$ (1I) calculated at M06/6-311++G(d,p) level. The *values in parentheses* and *brackets* are bond angles and Mulliken charges, respectively. The *values without parentheses* are distances in angstrom

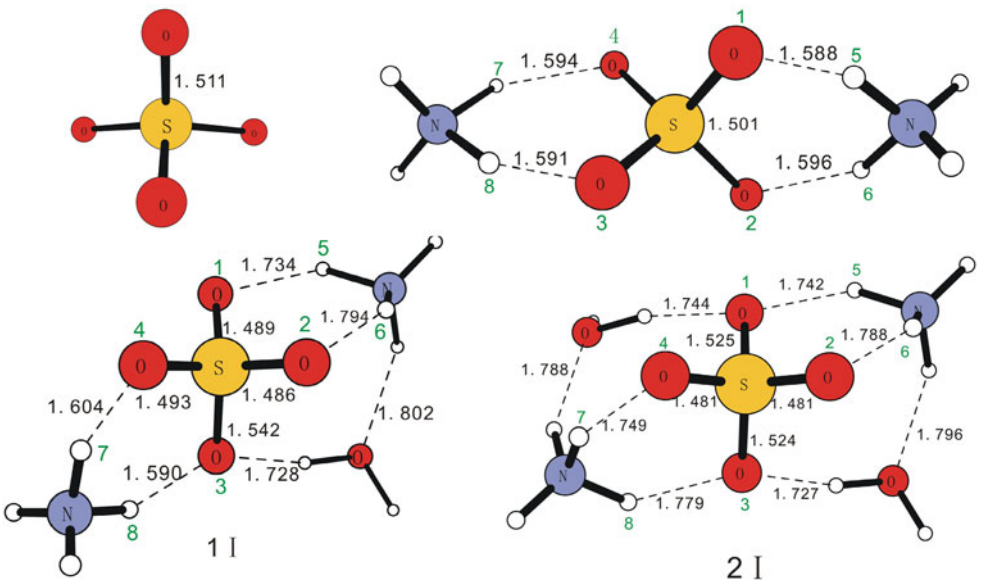

Fig. 3 Structures of SO_4^{2-} and $(NH_4)_2SO_4 \cdot (H_2O)_n$ ($n = 0$–2) calculated at M06/6-311++G(d,p) level. Bond lengths are in angstrom

shown in Fig. 3. In gas-phase $(NH_4)_2SO_4$, each oxygen of SO_4^{2-} anion is making a hydrogen bond to the NH moieties. The hydrogen-bond distances between NH_4^+ and SO_4^{2-} (R = 1.588–1.596 Å) are much smaller than the typical hydrogen-bond distance in water dimer (R = ~1.96 Å), indicating the strong electrostatic interaction between NH_4^+ and SO_4^{2-}. Compared to free NH_4^+ and SO_4^{2-}, the N–H bond is elongated by ~0.05 Å while the S–O bond is slightly shortened by ~0.01 Å, which is mainly caused by the dominant electrostatic interaction between NH_4^+ and SO_4^{2-}.

$(NH_4)_2SO_4 \cdot H_2O$: When an water molecule was added to the system, one stable conformation was located at the M06/6-311++G(d,p) level (denoted by structure 1I in Fig. 3). The most energetically privileged approach for the water molecule to $(NH_4)_2SO_4$ is via the formation of two additional hydrogen bonds. As shown in Fig. 3, the distance of the S–O bond, which is making a hydrogen bond to the introduced water, is elongated by 0.041 Å, while the other three SO bond lengths are hardly changed. The introduced water molecule acts as not only a proton donor but also a proton acceptor, leading to remarkable changes of hydrogen-bond distances (Fig. 3). Relative to $(NH_4)_2SO_4$, the hydrogen-bond distances R (H_5–O_1) and R (H_6–O_2) increase by 0.146 and 0.198 Å, respectively. This implies that the addition of water finally influences the electrostatic interaction between NH_4^+ and SO_4^{2-}. The charges of the related oxygen and hydrogen atoms are also changed when a water molecule is added. For example, the negative charge of the water–hydrogen-bonding oxygen is decreased from −0.47 to −0.41.

$(NH_4)_2SO_4 \cdot 2H_2O$: The cluster of $(NH_4)_2SO_4$ with two water molecules was optimized by adding H_2O to 1I. In the most stable configuration of the $(NH_4)_2SO_4 \cdot 2H_2O$ cluster (2I in Fig. 3), the added water forms two new hydrogen bonds between NH_4^+ and SO_4^{2-}. Other possible structures examined are less stable in energy. The distances of the remained hydrogen bonds (O_4–H_7 and O_3–H_8) are elongated to 1.749 and 1.779 Å, respectively. The significant increase in hydrogen-bond distances further demonstrate that the addition of water molecules indeed weakens the electrostatic interaction between NH_4^+ and SO_4^{2-}. In addition, the bond length of S–O_1 is lengthened by 0.036 Å due to the formation of the new hydrogen bond. Finally, it is worth noting that all water-involved hydrogen bonds are in the range of 1.727–1.802 Å.

$(NH_4)_2SO_4 \cdot nH_2O$ ($n = 3$–9): By adding water molecule into the system gradually, a number of low-energy configurations of the isomers have been found for the same substance at both M06/6-311++G(d,p) and B3LYP/6-311++G(d,p) levels. But, we only focus on the relatively stable structures even though other configurations probably exist in gas phase. Every three isomers of the same substance optimized at the M06/6-311++G(d,p) level are depicted in Fig. 4. It is clear that all structures are contact ion pairs (CIP) except 7II and 9III. The water in these clusters acts as not only proton donor but proton acceptor. With gradual increase in the number of water molecules, the structures of clusters transform from CIP to solvent-shared ion pairs (SIP).

As shown in Fig. 4, almost every NH_4^+ forms one hydrogen bond with SO_4^{2-} and two hydrogen bonds with H_2O. The hydrogen-bond distances of NH_4^+–SO_4^{2-} and NH_4^+–H_2O in $(NH_4)_2SO_4 \cdot nH_2O$ ($n = 2$–9) are listed in Fig. 5. Note that the difference in two hydrogen-bond distances between NH_4^+ and H_2O is in the range of 0–0.2 Å due to the changes of the NH_4^+ electron density, as more water molecules are integrated into this system.

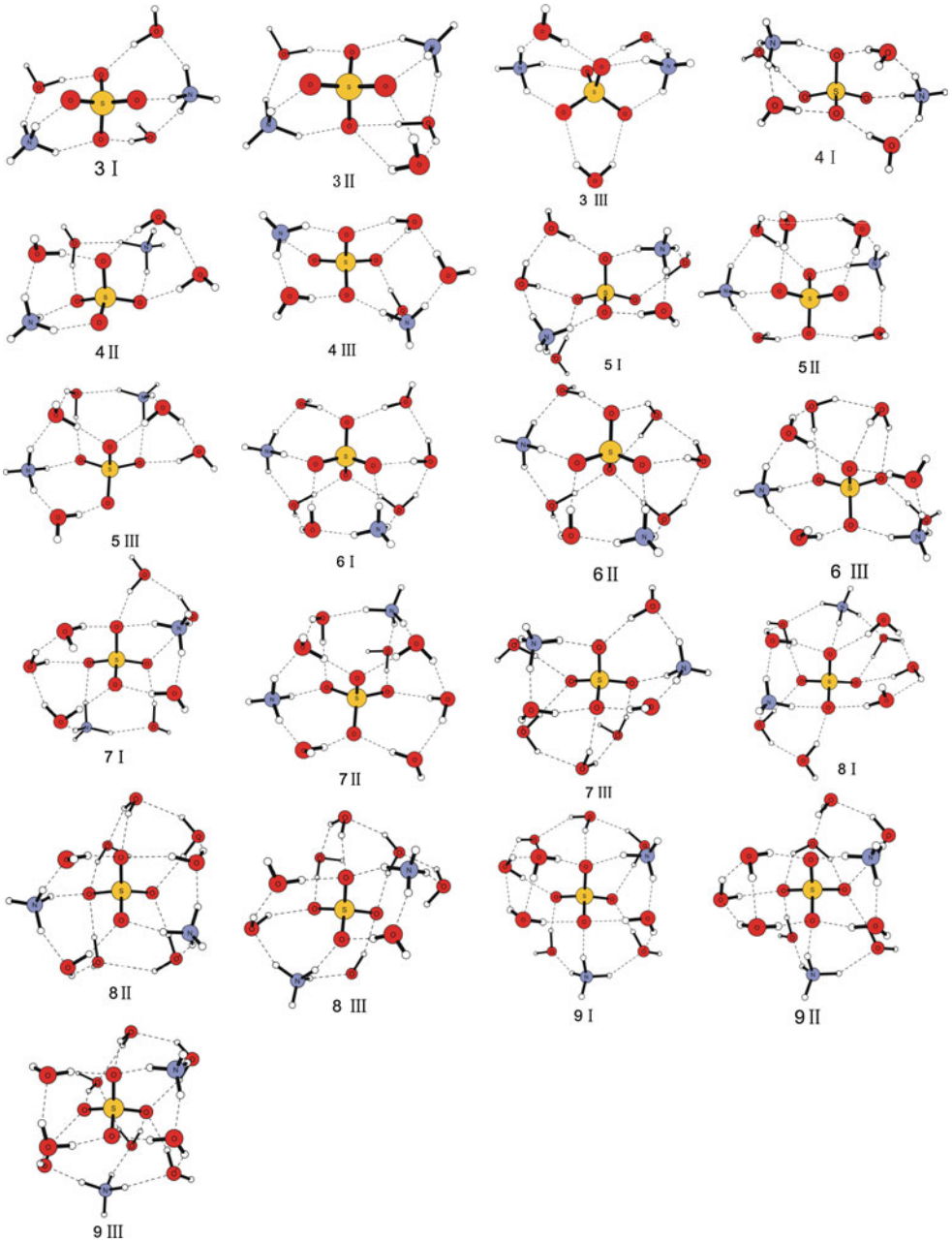

Fig. 4 Structures of $(NH_4)_2SO_4 \cdot (H_2O)_n$ ($n = 3$–9) calculated at M06/6-311++G(d,p) level

The hydrogen-bond distance between NH_4^+ and SO_4^{2-} is close to one of the other two hydrogen-bond distances between NH_4^+ and H_2O, which indicates that the interactions of NH_4^+–SO_4^{2-} and NH_4^+–H_2O are similar in gas phase for this system.

3.3 Binding energies

The total binding energy (ΔE_n) of the coupling of $(NH_4)_2SO_4 + nH_2O \rightarrow (NH_4)_2SO_4 \cdot (H_2O)_n$ and the stepwise binding energy ($\Delta E_{n-1,n}$) of $(NH_4)_2SO_4 \cdot (H_2O)_{n-1} + H_2O \rightarrow (NH_4)_2SO_4 \cdot (H_2O)_n$, where n increases from 1 to 9, are listed in Table 3. For each cluster, the binding energy is determined as the difference between the total energy of the cluster and the energy sum of isolated monomers contained in the cluster [55]. The ZPE corrections are considered to give the ZPE-corrected binding energies (ΔE_n^e and $\Delta E_{n-1,n}^e$), but no corrections are made for basis set superposition error in calculations as it can be ignored for bigger basis sets. It can be concluded that the formation of hydrogen bonds between $(NH_4)_2SO_4$ and H_2O contributes to the lowering of the system energy. In Table 3, the differences between ZPE-corrected and non-ZPE binding energies become larger with n increasing from 1 to 9, which indicates that, with the increment of water molecules, the system has higher zero-point vibration energies

Table 2 Relative energies (kcal/mol) of $(NH_4)_2SO_4 \cdot (H_2O)_n$ ($n = 0$–9) calculated at different theory levels

Species	M06		B3LYP	
	6-311++G(d,p)	Aug-cc-pvtz	6-311++G(d,p)	Aug-cc-pvtz
$(NH_4)_2SO_4$	95,945.31	95,944.88		
1I	47,972.80	47,972.99		
2I	0	0	0	0
3I	0	0	0	0
3II	2.68	2.42	5.61	5.42
3III	7.19	6.83	8.44	7.96
4I	0	0	0	0
4II	1.37	0.97	3.56	3.00
4III	3.18	3.00	3.68	2.67
5I	0	0	0.49	0.67
5II	1.29	0.69	0	0
5III	0.98	0.83	4.51	3.93
6I	0.10	0.64	0	0
6II	0	0	0.56	2.21
6III	1.36	1.19	0.99	2.32
7I	0.06	0.09	2.04	1.51
7II	0.16	1.04	0.94	1.30
7III	0	0	0	0
8I	0	0	0	0
8II	0.13	0.51	2.25	0.85
8III	4.15	3.40	1.69	2.24
9I	0	0	0	0
9II	9.47	8.51	5.33	7.15
9III	7.96	7.15	4.82	5.74

$(NH_4)_2SO_4 \cdot 2H_2O$ (2I) and the relatively most stable structure with the same number of water molecules set to zero for $(NH_4)_2SO_4 \cdot (H_2O)_n$ ($n = 0$–2) and $(NH_4)_2SO_4 \cdot (H_2O)_n$ ($n = 3$–9), respectively

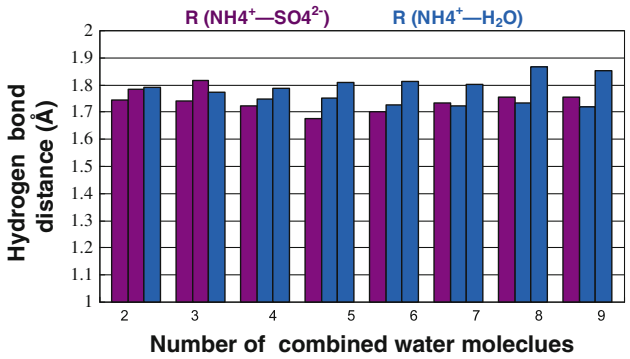

Fig. 5 The hydrogen-bond distance (Å) of $(NH_4)_2SO_4 \cdot (H_2O)_n$ ($n = 2$–9) calculated at M06/6-311++G(d,p) level

at 0 K. Note that the following discussion are made using the results with ZPE corrections.

The binding energy of $(NH_4)_2SO_4 + H_2O \rightarrow 1I$, which originates from the formation of two hydrogen bonds, is −15.69 kcal/mol (Table 3), a value that is lower than the typical hydrogen bonding energy of ~13 kcal/mol in water dimer [56]. In order to understand the role of water molecule in stabilizing the cluster, the charge distribution of 1I is given in Fig. 2. The negative charge of an oxygen atom in SO_4^{2-} increases by 0.24 attributed to forming hydrogen bond with H_2O. This means that H_2O has a strong interaction with SO_4^{2-} and NH_4^+ and provides efficient stabilization of the whole cluster [33]. In structure 2I, the binding energy ($1I + H_2O \rightarrow 2I$) is −16.94 kcal/mol, which reflects that the second water molecule plays the same important role in stabilizing the system. It was found that SO_4^{2-}, which was not stable as an isolated species, could be stabilized by at least three hydrated water molecules in gas phase [44]. When two water molecules are added into $(NH_4)_2SO_4$, the total binding energy with four additional hydrogen bonds is −32.63 kcal/mol, a value that significantly exceeds the energy barrier of the $(NH_4)_2SO_4$ formation (13.60 kcal/mol, Fig. 1) as described above. Therefore, it can be concluded that two water molecules could definitely stabilize the $(NH_4)_2SO_4$ monomer.

After adding H_2O to 2I, three isomers (3I, 3II, and 3III) are produced with three different kinds of hydrogen bonds formed. The stepwise binding energies of 3I, 3II, and 3III considerably differ from each other with a deviation larger than 2% (Table 3). It is found that the increase in

Table 3 Total and stepwise binding energies (kcal/mol) of $(NH_4)_2SO_4 + nH_2O \rightarrow (NH_4)_2SO_4 \cdot (H_2O)_n$ and $(NH_4)_2SO_4 \cdot (H_2O)_{n-1} + H_2O \rightarrow (NH_4)_2SO_4 \cdot (H_2O)_n$ calculated at M06/6-311++G(d,p) level

Species	$-\Delta E_n$	$-\Delta E_{n-1,\ n}$	$-\Delta E_n^e$	$-\Delta E_{n-1,\ n}^e$
1I	19.42		15.69	
2I	38.91	19.45 (1I)	32.63	16.94 (1I)
3I	56.48	17.57 (2I)	47.69	15.06 (2I)
3II	53.97	15.06 (2I)	44.55	11.92 (2I)
3III	48.95	10.04 (2I)	40.79	8.16 (2I)
4I	72.79	16.32 (3I)	60.87	13.19 (3I)
4II	71.54	15.06 (3I)	58.98	11.29 (3I)
4III	69.65	15.69 (3III)	58.36	13.81 (3III)
5I	88.48	15.69 (4II)	73.42	14.43 (4II)
5II	87.22	14.43 (4I)	72.16	11.29 (4I)
5III	87.22	14.43 (4I)	73.42	12.55 (4I)
6I	101.66	13.18 (5I)	84.71	11.29 (5I)
6II	101.66	13.18 (5I)	84.09	10.67 (5I)
6III	101.66		84.71	
7I	114.83	13.19 (6II)	94.13	10.67 (6II)
7II	114.83	13.18 (6III)	94.13	11.92 (6III)
7III	114.83		94.13	
8I	126.13	11.29 (7II)	104.17	9.41 (7II)
8II	125.50	10.67 (7II)	103.54	8.79 (7II)
8III	122.36	7.53 (7III)	100.40	5.65 (7III)
9I	143.07		117.34	
9II	133.66	8.16 (8II)	109.81	6.28 (8II)
9III	134.91	8.79 (8I)	109.81	5.65 (8I)

[e] With ZPE correction

$\Delta E_{n-1,n}^e$ depends on the position of the third water molecule. The most stable configuration in $(NH_4)_2SO_4 \cdot (H_2O)_3$ is 3I, in which the third water molecule not only interacts with SO_4^{2-} but also with NH_4^+. This is a common feature that can be observed in other clusters. In addition, the average binding energy, $\Delta E_{n-1,n}^e$ ($n = 1$–9), is increased from −16.94 to −5.65 kcal/mol, showing that the interaction between $(NH_4)_2SO_4$ and H_2O is the dominant intermolecular interaction in the present system.

3.4 Dynamic process of the transformation between solvent-shared ion pairs and contact ion pairs

It is interesting to notice that the energy difference between 7I and 7II is very small (see Table 2) but a large discrepancy in geometry can be observed (Fig. 4). Both of NH_4^+ cations are interacting with SO_4^{2-} directly in the form of CIP of 7I, but, in 7II, there is a water molecule between SO_4^{2-} and one of NH_4^+, which is known as solvent separated ion pair. In order to understand the relationship between these two different configurations, the first principle MD method was used to simulate microscopic process of structural transformation with 7I as an initial configuration.

The effect of structural change on energy evolution is shown in Fig. 6a, and the representative snapshots (A–E) at 0, 2.959, 6.766, 22.534, and 27.994 ps are given in Fig. 6b. Among these structures, (A) and (E) are similar to 7I while the others resemble 7II. As described in Fig. 4, each NH_4^+ forms one hydrogen bond with SO_4^{2-} and two hydrogen bonds with H_2O in the cluster of 7I. However, in 7II, only one NH_4^+ has the same interaction and the other associates with three water molecules. The hydrogen-bond distance R (NH_4^+–SO_4^{2-}) and relative energies of the above six typical configurations are all listed in Table 4, where the energy of structure A (7I) is chosen to be zero. It is clear that the relative energy is always oscillating within the range of 0–3.77 kcal/mol. The maximum energy difference is 3.77 kcal/mol, which results from the transformation of hydrogen-bond network among SO_4^{2-}, NH_4^+, and H_2O. Furthermore, it can be observed that the hydrogen-bond replacement of NH_4^+–SO_4^{2-} by NH_4^+–H_2O and SO_4^{2-}–H_2O has already been accomplished within 3 ps, which is consistent with the residence time of 4.6 ± 0.3 ps for H_2O–H_2O [57, 58]. This is probably attributed to the competition among the interactions of NH_4^+–SO_4^{2-}, NH_4^+–H_2O, and SO_4^{2-}–H_2O.

3.5 Vibration frequencies

The harmonic vibration frequencies of symmetric stretching of SO_4^{2-} (υ_1-SO_4^{2-}) in $(NH_4)_2SO_4 \cdot (H_2O)_n$ ($n = 2$–9) obtained at the M06/6-311++G(d,p), B3LYP/6-311++G(d,p), and HF/6-311++G(d,p) levels, respectively (see Table 5). The experimental frequencies for some clusters are also listed in Table 5. The mean deviation of the M06 calculations from experimental results is the smallest among these methods. As presented in Table 5, the SO_4^{2-} symmetric stretching frequencies calculated by B3LYP are underestimated by ~80 cm^{-1}, while harmonic frequencies calculated by HF are apparently overestimated by as much as 80 cm^{-1}. The deviations of the B3LYP and HF values are within 8% of the available experiment values. The harmonic frequencies calculated by M06 are in better agreement with experimental values than those obtained by B3LYP and HF. These results indicate that M06 is a more accurate functional than B3LYP for the present system. The M06 results are thus used in the following discussion.

The symmetric stretching frequency of SO_4^{2-} (υ_1-SO_4^{2-}) is expected to be sensitive to the surrounding environment, such as cation type and salt concentrations. For example, in $MgSO_4 \cdot (H_2O)_n$ system, symmetric stretching frequency of SO_4^{2-} was found to undergo a maximum shift of 53 cm^{-1}

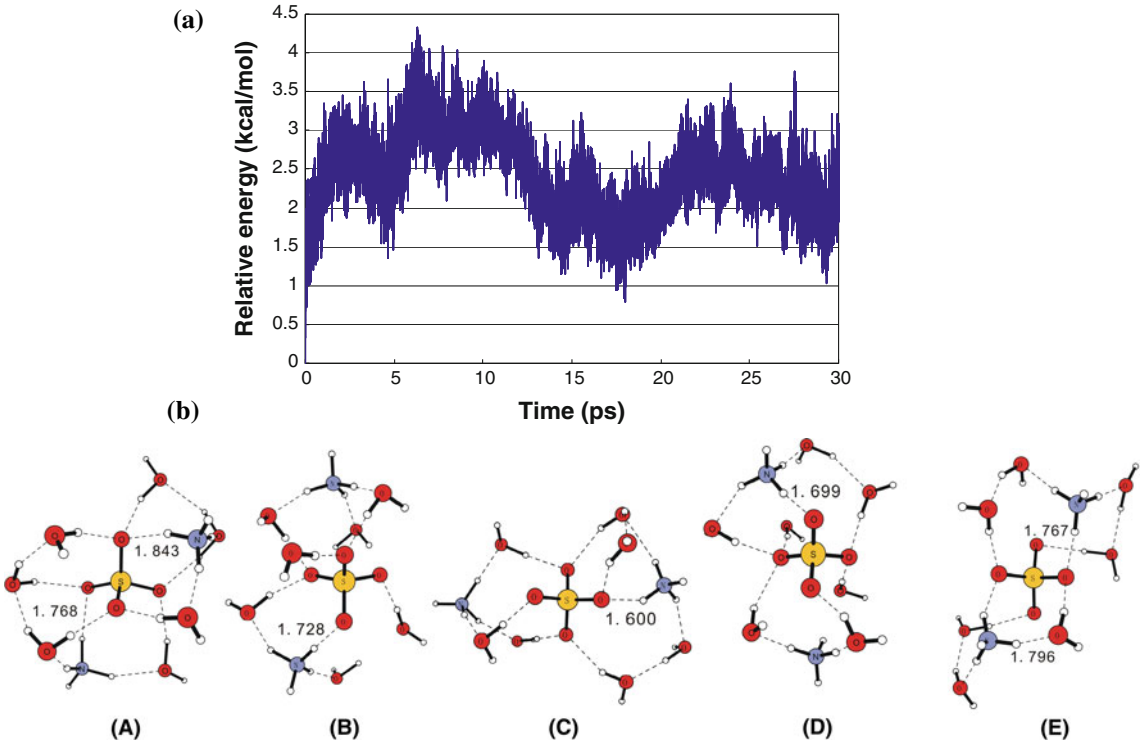

Fig. 6 **a** Time evolution of the energy changes at 298 K. **b** The snapshots (*A–E*) at 0, 2.959, 6.766, 22.534 and 27.994 ps, respectively. Bond lengths are in angstrom

Table 4 The hydrogen-bond distance R (NH_4^+–SO_4^{2-}) (Å) and relative energies (kcal/mol) of the representative configurations A–E and 7II at 298 K

Snapshots	Time (ps)	R (NH_4^+–SO_4^{2-})	R (NH_4^+–SO_4^{2-})	Relative energies
A (7I)	0	1.843	1.768	0
B	2.959		1.728	2.51
C	6.766		1.600	3.14
D	22.534		1.699	2.51
E	27.994	1.796	1.767	1.26
7II			1.661	2.51

The energy of structure A (7I) is set to zero for reference

(from 953 to 1,006 cm^{-1}), when $MgSO_4$ forming various ion pairs with different water molecules [59]. It demonstrates that the interaction between SO_4^{2-} and Mg^{2+} is much stronger than that between SO_4^{2-} and H_2O. For the hydrated $(NH_4)_2SO_4$ system, the υ_1-SO_4^{2-} frequencies of 3I–3III are 960, 952, and 945 cm^{-1}, respectively, undergoing a red shift of 13 and 5 cm^{-1} and a blue shift of 2 cm^{-1} compared to that of 2I (Table 5). Depending on how the hydrogen bond is integrated in $(NH_4)_2SO_4 \cdot (H_2O)_n$ where n increases from 4 to 9, the frequencies spread over the range of 956–973 cm^{-1} for all isomers. Compared to that of $MgSO_4$ system, this fluctuation range is obviously small with the change in the number of the water molecule. It can thus be concluded that interactions of NH_4^+–SO_4^{2-}, NH_4^+–H_2O, and SO_4^{2-}–H_2O are similar in gas phase, which are in line with the conclusion obtained by the first principle MD.

4 Conclusions

The reaction of sulfuric acid (H_2SO_4) and ammonia (NH_3) in the absence of water molecule has been investigated with M06 method. It indicates that $(NH_4)_2SO_4$ and NH_4HSO_4 may exist in very shallow minima in gas phase, which is a theoretical prediction and requires to be further detected in experiment. Equilibrium structures, harmonic frequencies, and binding energies of $(NH_4)_2SO_4 \cdot (H_2O)_n$ ($n = 0$–9) have been obtained using both M06 and B3LYP methods. The analyses of the selected equilibrium bond lengths and hydrogen-bond lengths indicate that the formation of hydrogen bonds between ions and water molecules lengthens the bond lengths due to the decrement of electrostatic interaction and charges transfer. The stepwise binding energies $\Delta E^e_{n-1,n}$ decrease gradually with n increasing from 2 to 9, indicating that the interaction strength between ions and water molecules is stronger than that between solvent molecules. However, the interaction between NH_4^+ and H_2O is comparable to that between SO_4^{2-} and H_2O.

Table 5 Frequencies of the υ_1-SO_4^{2-} of $(NH_4)_2SO_4 \cdot (H_2O)_n$ calculated at M06/6-311++G(d,p), B3LYP/6-311++G(d,p) and HF/6-311++G(d,p) levels, respectively, and compared with the corresponding experimental results

Species	M06	B3LYP	HF	Experiments
2I	947	866	1,036	
3I	960	887	1,048	
3II	952	862	1,040	
3III	945	883	1,040	
4I	969	895	1,052	
4II	961	899	1,050	979
4III	956	885	1,044	
5I	966	904	1,054	
5II	960	895	1,055	979
5III	970	900	1,052	
6I	969	908	1,056	
6II	957	910	1,056	979
6III	965	910	1,054	
7I	971	908	1,058	
7II	973	911	1,058	979
7III	972	917	1,059	
8I	971	902	1,057	
8II	968	906	1,059	979
8III	969	914	1,057	
9I	968	903	1,056	
9II	969	905		979
9III	971	907	1,056	

We have also studied the dependence of the SO_4^{2-} symmetric stretching shifts on the number of water molecules in $(NH_4)_2SO_4 \cdot (H_2O)_n$ ($n = 0$–9). The results show that υ_1-SO_4^{2-} does not change substantially as $n \geq 4$. Compared with B3LYP, M06 is a better functional used in calculating the harmonic frequencies for the present system. The M06 functional is expected to be applicable to deal with the non-covalent interactions. Our calculations demonstrate that equilibrium structures, harmonic frequencies, and interaction energies of $(NH_4)_2SO_4 \cdot (H_2O)_n$ ($n = 0$–9) are predominantly governed by electrostatic interactions. Moreover, the first principle molecular dynamics method was used to simulate structural transformation of two representative isomers whose energies are close. The results show that the interactions of NH_4^+–SO_4^{2-}, NH_4^+–H_2O, and SO_4^{2-}–H_2O are similar, which is consistent with the results obtained by vibration frequencies. These theoretical results may further improve our understanding toward diverse interactions in the present system.

Acknowledgments This work is supported by the Major State Basic Research Development Programs (2011CBA00701), the National Natural Science Foundation of China (20933001, 20873006, 20904007, and 21103010), the 111 Project B07012, the Excellent Young Scholars Research Fund of Beijing Institute of Technology (2010Y1214), and the Basic Research Fund of Beijing Institute of Technology (20101742032). We thank Dr. Sven de Marothy (Stockholm University) for providing graphical program used to make Figs. 2, 3, 4, and 6b in this paper.

References

1. Coakley JAJ, Cess RD, Yurevich FB (1983) J Atmos Sci 40:116–138
2. Charlson RJ, Langner J, Andreae MO, Warren SG (1991) Tellus 43:152–163
3. Pincus R, Baker MB (1994) Nature 372:250
4. See the special issue of Faraday Discuss (1996) 103
5. Meot-Ner M (1984) J Am Chem Soc 106:1265
6. Lisy JM (1997) Int Rev Phys Chem 16:267
7. Wang YS, Jiang JC, Cheng CL, Lin SH, Lee YT, Chang HC (1997) J Chem Phys 107:9695
8. Wang YS, Chang HC, Jiang JC, Lin SH, Lee YT (1998) J Am Chem Soc 102:8777
9. Fox BS, Beyer MK, Bondbey VE (2001) J Phys Chem A 105:6386
10. Diken EG, Hammer NI, Johnson MA, Christie RA, Jordan KD (2005) J Chem Phys 123:164309
11. Azeim SA, Van der Rest G (2005) J Phys Chem A 109:2505
12. Pankewitz T, Lagutschenkov A, Niedner-Schatteburg G, Xantheas SS, Lee YT (2007) J Chem Phys 126:074307
13. Bagno A, Conte V, Furia FD, Moro S (1997) J Phys Chem A 101:4637
14. Douady J, Calvo F, Spiegelman F (2008) J Chem Phys 129:154305
15. Wang YS, Chang HC, Jiang JC, Lin SH, Lee YT (1998) J Am Chem Soc 120:8777
16. Khan A (2001) Chem Phys Lett 338:201
17. Bruge F, Bernasconi M, Parrinello M (1999) J Chem Phys 110:4734
18. Pickard FC, Dunn ME, Shields GC (2005) J Phys Chem A 109:4905
19. Lee HM, Tarakeshwar P, Park J, Kolaski MR, Yoon YJ, Yi H, Kim WY, Kim KS (2004) J Phys Chem A 108:2949
20. Karthikeyan S, Singh JN, Park M, Kumar R, Kim KS (2008) J Chem Phys 128:44304
21. Contador JC, Aguilar MA, Olivares del Valle F (1997) J Chem Phys 214:113
22. Bueker HH, Uggered E (1995) J Phys Chem 99:5945
23. Glendening ED, Feller D (1995) J Phys Chem 99:3060
24. Magnusson E (1994) J Phys Chem 98:12558
25. Kim J, Lee S, Cho SJ, Mhin BJ, Kim KS (1995) J Chem Phys 102:839
26. Bauschlicher CW, Langhoff SR, Partridge H, Rice JE, Komornicki A (1991) J Chem Phys 95:5142
27. Feller D, Glendening ED, Kendall RA, Peterson KA (1994) J Chem Phys 100:4981
28. Xie Y, Remington RB, Schaefer HF (1994) J Chem Phys 101:4878
29. Bagno A, Conte V, Furia FD, Moro S (1997) J Phys Chem A 101:4637
30. Jiang JC, Chang HC, Lee YT, Lin SH (1999) J Phys Chem A 103:3123
31. Larson LJ, Largent A, Tao FM (1999) J Phys Chem A 103:6786
32. Anderson KE, Siepmann JI, McMurry PH, VandeVondele J (2008) J Am Chem Soc 130:14144

33. Zhao YY, Zeng EY, Zhang XH, Ma L, Tao FM (2010) Chin J Struct Chem 29:525–534
34. Zhao J, Khalizov AF, Zhang R, McGraw R (2009) J Phys Chem 113:680–689
35. Kurten T, Torpo L, Sundberg MR, Kerminen VM, Vehkamaki H, Kulmala M (2007) Atmos Chem Phys 7:2765–2773
36. Zhang R, Suh I, Zhao J, Zhang D, Fortner EC, Tie X, Molina LT, Molina MJ (2004) Science 304:1487–1490
37. Nadykto AB, Yu FQ (2007) Chem Phys Lett 435:14
38. Zhang R, Wang L, Khalizov AF, Zhao J, Zheng J, McGraw RL, Molina LT (2009) Proc Natl Acad Sci 106:17650–17654
39. Nadykto AB, Yu F (2007) Chem Phys Lett 435:14–18
40. Kurten T, Torpo L, Ding CG, Vehkamaki H, Sundberg MR, Laasonen K, Kulmala M (2007) J Geophys Res 112:D04210
41. Nadykto AB, Natsheh AA, Yu F, Mikkelsen KV (2008) Adv Quantum Chem 55:449–478
42. Kurten T, Vehkamaki H (2008) Adv Quantum Chem 55:407–427
43. Friend JP, Feeley HW, Krey PW, Spar J, Walton A (1961) The high altitude sampling program, Vol 5 Supplementary HASP studies, vol 5. Defense Atomic Support Agency, Washington, DC
44. Wang XB, Nicholas JB, Wang LS (2000) J Chem Phys 113:10837
45. Dong JL, Li XH, Zhao LJ, Xiao HS, Wang F, Guo X, Zhang YH (2007) J Phys Chem B 111:12170–12176
46. Frisch MJ, Trucks GW et al (2009) Gaussian 09 revision a.l. Gaussian Inc, Wallingford
47. Zhao Y, Truhlar DG (2008) Theor Chem Acc 120:215
48. Becke AD (1993) J Chem Phys 98:5648
49. Perdew JP, Burke K, Ernzerhof M (1996) Phys Rev Lett 77:3865
50. Delley B (2000) J Chem Phys 113:7756–7764
51. Delley B (1990) J Chem Phys 92:508–517
52. Novoa JJ, Sosa C (1995) J Phys Chem 99:15837
53. Dahlke EE, Orthmeyer MA, Truhlar DG (2008) J Phys Chem B 112:2372–2381
54. Bryantsev VS, Diallo MS, Van duin ACT, Goddard WA (2009) J Chem Theory Comput 5:1016–1026
55. Larson LJ, Largent A, Tao FM (1999) J Phys Chem A 103:6786–6792
56. Rablen PR, Lockman JW, Jorgensen WL (1998) J Phys Chem A 102:3782
57. Zhang YH, Chan CK (2003) J Phys Chem A 107:5956–5962
58. Ohtaki H (2001) Monatshefte für Chemie 132:1237–1268
59. Zhang H, Zhang YH, Wang F (2009) J Comput Chem 30:493–503